Supporting Information

Proton-Coupled Electron Transfer Driven by Coordination-Induced Bond Weakening at a Trivalent Uranium Center

I.J. Huerfano, Tate M. Quinn, Ahmed Kangmennaa, Matthias Zeller and Suzanne C. Bart*

H.C. Brown Laboratory, James Tarpo Jr. and Margaret Tarpo Department of Chemistry, Purdue University
560 Oval Drive West Lafayette, Indiana 47907-2084

Table of Contents

Experimental. S3

General Considerations. S3

Bond Dissociation Free Energy Bracketing Experiments. S3

Synthesis of Cationic Uranium Complexes. S4

pK_a Bracketing Experiments. S5

Electrochemical Data. S5

NMR Spectral Data. S6

FT-IR Spectroscopic Data. S18

Electronic Spectral Data. S18

Crystallographic Information. S19

References S21

Experimental.

General Considerations. All manipulations were performed under an atmosphere of argon using standard Schlenk techniques or in an MBraun dry box with an atmosphere of purified nitrogen. Glassware was oven-dried at 150 °C overnight or flame dried prior to use. Solvents were purchased from commercial sources, purified and degassed using a Seca solvent purification system or dried by conventional methods and degassed by three freeze-pump-thaw cycles. Solvents were stored over activated 4 Å molecular sieves and sodium metal in the dry box prior to use. Benzene-d_6 and pyridine-d_5 were purchased from Cambridge Isotope Laboratories, dried with 4 Å molecular sieves and sodium, then degassed by five freeze−pump−thaw cycles. All starting reagents were commercially available and used without further purification unless otherwise noted. Tp*$_2$UI,[1] Tp*$_2$UBn,[2] Tp*$_2$UNHTol (**1**),[3] $NaBArF_{24}$,[4] $[Cp_2Co]BArF_{24}$,[5] Cp*Rh(2-PyPh)H,[6] Gomberg's Dimer,[7] and •OMes*[8] were synthesized according to reported literature procedures.

Caution! U-238 is a weak α-emitter with a half-life of $t_{1/2} = 4 \times 10^9$ years.

^{1}H-NMR, ^{11}B{^{1}H}-NMR, and ^{19}F{^{1}H}-NMR spectra were collected at 25 °C on either a Bruker AV-III-400-HD or Bruker NEO500-1 spectrometer. All ^{1}H chemical shifts are reported relative to $SiMe_4$, using the residual proteo-solvent impurity as a standard. ^{11}B-NMR chemical shifts are reported relative to the peak for $BF_3{\cdot}Et_2O$. Electronic absorption spectroscopic measurements were recorded at 294 K in sealed 1 cm quartz cuvettes with a Cary 6000i UV−vis/NIR spectrophotometer. FT-infrared spectra were recorded using a Thermo Nicolet iS5 spectrometer. Electrochemical analysis was performed using a CH Instruments CHI660E Electrochemical Workstation. Cyclic Voltammetry and Differential Pulse Voltammetry were completed using a glassy carbon working electrode, platinum coil counter electrode, and a Ag/AgCl reference electrode. 0.1 M TBA(BPh_4) was employed as a supporting electrolyte in THF. All CVs are referenced to an external Fc/Fc$^+$ standard.

A red brown, plate-shaped crystal was mounted on the goniometer. Data for **4** were collected from a shock-cooled single crystal at 150(2) K on a Bruker AXS D8 Quest four circle diffractometer with an I-mu-S 3.0 microsource X-ray tube with HELIOS multilayer Montel optics for monochromatization and a PhotonIII_C14 charge-integrating and photon counting pixel array detector. The diffractometer used CuK_α radiation (λ = 1.54178 Å). All data were integrated with SAINT V8.41 and a numerical absorption correction using SADABS 2016/2 was applied.[9,10] The structure was solved by dual methods with SHELXT and refined by full-matrix least-squares methods against F^2 using SHELXL-2025/1.[11,12] All non-hydrogen atoms were refined with anisotropic displacement parameters. All hydrogen atoms were refined with isotropic displacement parameters. Some of their coordinates were refined freely and some on calculated positions using a riding model with their U_{iso} values constrained to 1.5 times the U_{eq} of their pivot atoms for terminal sp^3 carbon atoms and 1.2 times for all other carbon atoms. Disordered moieties were refined using bond lengths restraints and displacement parameter restraints (see Refinement details for **4** in the Crystallographic Information section). Crystallographic data for **4** have been deposited with the Cambridge Crystallographic Data Centre.[13] CCDC **2530055** contains the supplementary crystallographic data. These data can be obtained free of charge from The Cambridge Crystallographic Data Centre via www.ccdc.cam.ac.uk/structures.

Bond Dissociation Free Energy Bracketing Experiments.

Reaction of 1 with •OMes*. In separate 20 mL scintillation vials, 35 mg •OMes* (0.136 mmol) and 106 mg **1** (0.113 mmol) were dissolved in 3 mL of THF each and cooled to −35 °C. The solution of •OMes* was then added dropwise to the solution of **1** resulting in an immediate color change to red. The reaction mixture was stirred for 1 hour while warming to room temperature. The solvent was then removed in *vacuo,* and the product washed with cold pentane (3 x 5 mL) to give Tp*$_2$UNTol (**2**) as a dark red solid (83 mg; 79% yield). Characterization data is consistent with the previously reported synthesis.[14]

Reaction of 1 with Gomberg's Dimer. In separate 1-dram vials, 7 mg Gomberg's Dimer (0.014 mmol; 1 eq. trityl radical) and 26 mg **1** (0.028 mmol) were dissolved in approximately 0.5 mL C_6D_6. The two solutions were added together, transferred to an NMR tube outfitted with a Teflon J. Young valve, and allowed to react for 1 hour at room temperature. NMR data collected after 1 hour reveals complete conversion to **2** and triphenyl methane.

Reaction of 1 with Azobenzene. Conducted analogously to the procedure with Gomberg's dimer using 5 mg azobenzene (0.028mmol; 2 hydrogens per azobenzene) and 52 mg **1** (0.055 mmol). NMR data collected after 2 hours reveals complete conversion to approximately a 9:1 mixture of **2** and $Tp^*_2U(N_2Ph_2)$ (**3**)[15] with some minor boron-containing impurities.

Reaction of 2 with Diphenyl Hydrazine. 15 mg diphenyl hydrazine (0.080 mmol) were added to 15 mg of **2** (0.016 mmol) in C_6D_6 at room temperature. The reaction was allowed to sit unperturbed for 18 hours at room temperature, resulting in a dark brown solution. NMR spectral data is consistent with a mixture of **2** and **3** in approximately a 9:1 ratio.

Attempted Reaction of 2 with Cp*Rh(2-PyPh)H. 10 mg Cp*Rh(2-PyPh)H (0.025 mmol) and 24 mg of **2** (0.026 mmol) were dissolved in approximately 0.5 mL C_6D_6 at room temperature. The reaction mixture was monitored by NMR for 18 hours at room temperature then an additional 18 hours at 80 °C. No reaction was observed.

Synthesis of Cationic Uranium Complexes.

Synthesis of $[Tp^*_2UNHTol]BArF_{24} \bullet 2\ C_5H_{12}$ (4). In separate 20 mL scintillation vials, 40 mg **1** (0.043 mmol) and 45 mg $[Cp_2Co]BArF_{24}$ (0.043 mmol) were dissolved in 3 mL of THF each and cooled to −35 °C. The solution of **1** was then added to the solution of $[Cp_2Co]BArF_{24}$ resulting in an immediate color change to red-brown. The reaction mixture was stirred for 1 hour while warming to room temperature. The solvent was then removed in *vacuo,* and the product washed with pentane (3 x 5 mL) to remove cobaltocene and give $[Tp^*_2UNHTol]BArF_{24} \bullet 2\ C_5H_{12}$ (**4**) as a dark red-brown solid (55 mg; 66% yield). ^{1}H-NMR (400.13 MHz, 26 °C, C_6D_6) δ = −7.69 (br, 18H), 6.35 (v. br, 18H), 7.50 (s, 4H), 8.13 (s, 8H), 23.69 (s, 3H), 32.38 (br, 2H), 49.75 (br, 2H) ppm; ^{11}B{^{1}H}-NMR (128.38 MHz, 26 °C, C_6D_6) δ = −81.35, −6.56 ppm; ^{19}F{^{1}H}-NMR (376.50 MHz, 26 °C, C_6D_6) δ = −64.20 ppm. FT-IR (KBr): 2563 cm^{-1} (B-H), 3432 cm^{-1} (N-H). UV-Vis/NIR: λ_{max} = 436 nm (ε = 2200 $M^{-1}\ cm^{-1}$) and 500 nm (ε = 1300 $M^{-1}\ cm^{-1}$).

Attempted Reaction of 1 with $AgBPh_4$. In a 20 mL scintillation vial, 30 mg **1** (0.032 mmol) was dissolved in 2 mL of toluene. A suspension of $AgBPh_4$ (14 mg, 0.033 mmol) in 4 mL of toluene was then added giving a color change to dark brown. The reaction mixture was stirred for two hours at room temperature, filtered through a pad of celite, and solvent removed in *vacuo*. The resulting red solid was determined to contain primarily **2** and our previously reported Tp^*_2UO[16] in approximately a 7:3 ratio by NMR.

Independent Synthesis of $[Tp^*_2U]BArF_{24}$ (5). In a 20 mL scintillation vial, 50 mg Tp^*_2UI (0.052 mmol) was dissolved in 3 mL of diethyl ether. A solution containing 46 mg $NaBArF_{24}$ (0.052 mmol) in 3 mL diethyl ether was then added resulting in a color change to bright blue and precipitation of a white solid. The reaction mixture was stirred for 1 hour at room temperature, filtered through a pad of celite, and solvent was removed in *vacuo*. The resulting blue residue was triturated with pentane then dried in *vacuo* for 1 hour to remove coordinated solvent giving **5** as a bright blue solid (72 mg, 77% yield). Compound **5** only exhibits solubility in coordinating solvents such as diethyl ether, THF, and pyridine, presumably through adduct formation. The identity of **5** was supported by single-crystal X-ray diffraction. The data was of poor quality, allowing for determination of connectivity only (Figure S29). ^{1}H-NMR (400.13 MHz, 26 °C, THF-d_8) δ = −13.70 (br, 18H), 2.54 (br, 18H), 7.57 (s, 4H), 7.79 (s, 8H), 8.42 (s, 6H) ppm; ^{11}B{^{1}H}-NMR (128.38 MHz, 26 °C, THF-

d_8) δ = −6.89, 14.20 ppm; $^{19}F\{^1H\}$-NMR (376.50 MHz, 26 °C, THF-d_8) δ = −64.97 ppm. UV-Vis/NIR: λ_{max} = 585 nm (ε = 878 M^{-1} cm^{-1}) and 616 nm (ε = 823 M^{-1} cm^{-1}).

pK_a Bracketing Experiments.

General Procedure. In separate 1-dram vials, 15 mg **4** (0.083 mmol) and excess base (3-10 equivalents) were dissolved in approximately 0.5 mL C_6D_6. The two solutions were added together, transferred to an NMR tube outfitted with a Teflon J. Young valve, and allowed to equilibrate overnight at room temperature.

Electrochemical Data.

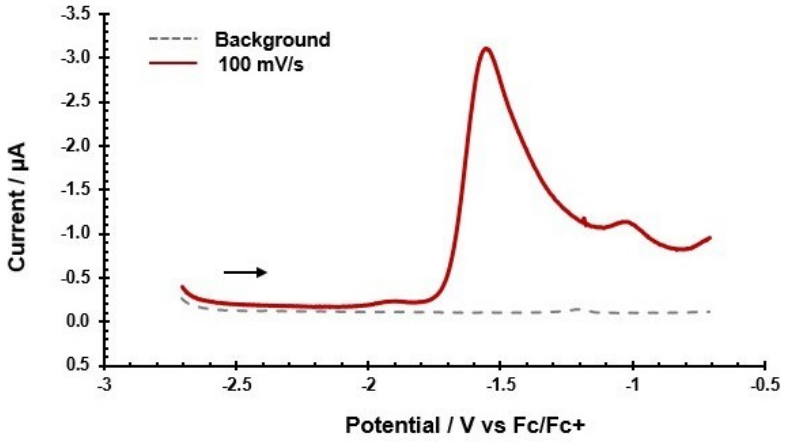

Figure S1. Differential Pulse Voltammogram data for **1**. 4 mM **1**; 0.1 M TBA(BPh_4)/THF; Glassy Carbon Working Electrode/Platinum Coil Counter Electrode; Ag/AgCl Reference Electrode.

NMR Spectral Data.

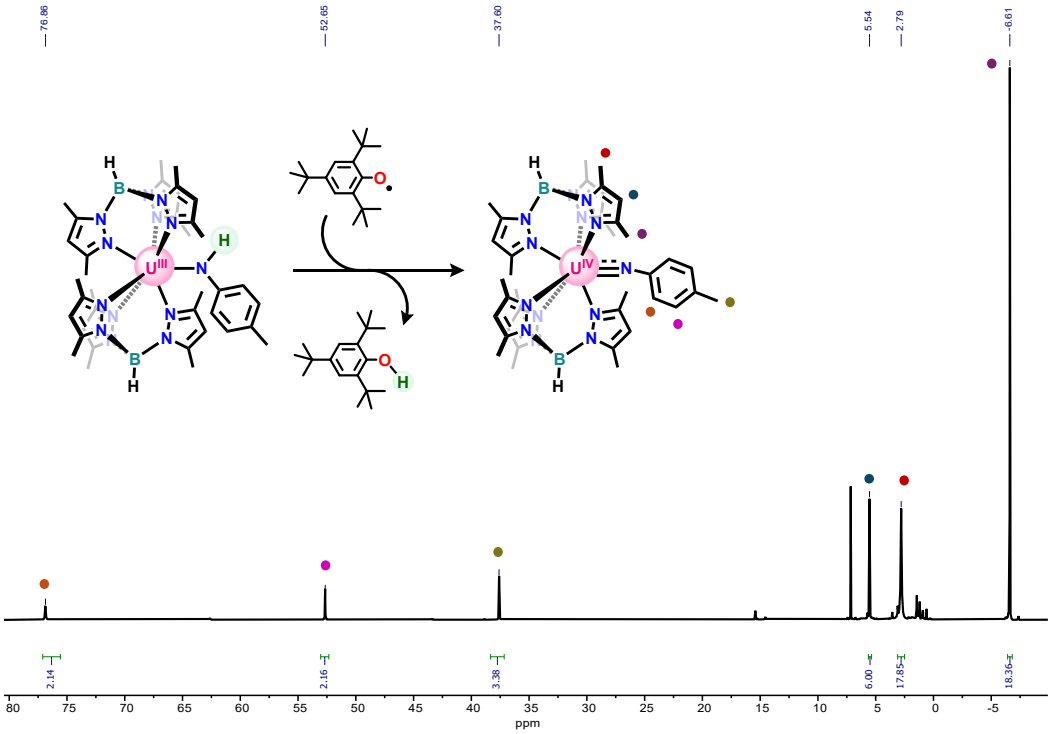

Figure S2. ^{1}H-NMR Spectrum (500.13 MHz, 26 °C, C_6D_6) of isolated **2** from reaction with •OMes*.

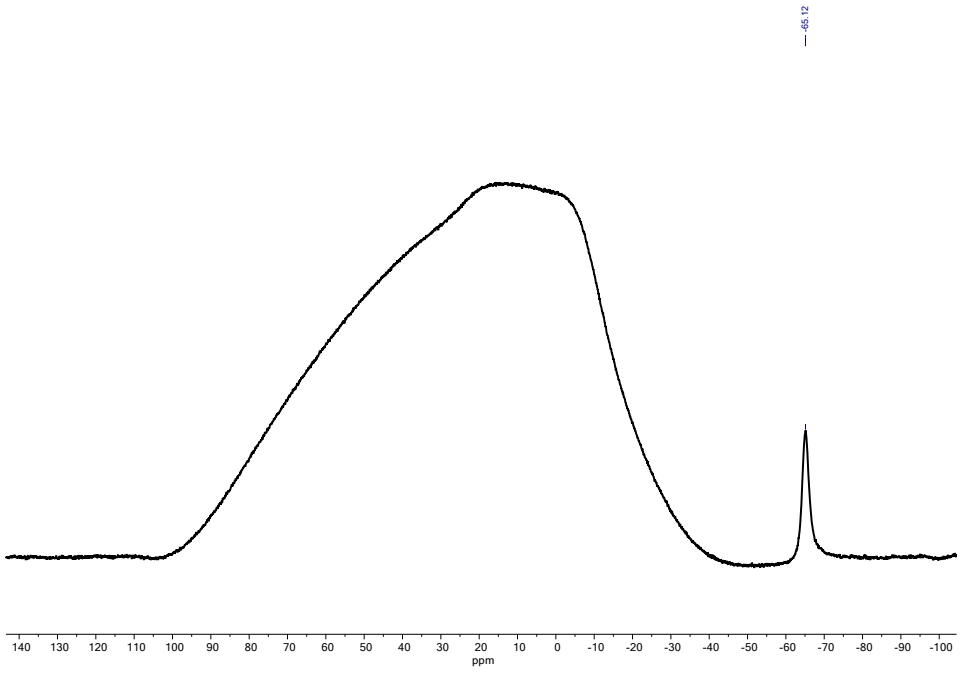

Figure S3. ^{11}B{^{1}H}-NMR Spectrum (160.46 MHz, 26 °C, C_6D_6) of the reaction of **1** with Gomberg's Dimer.

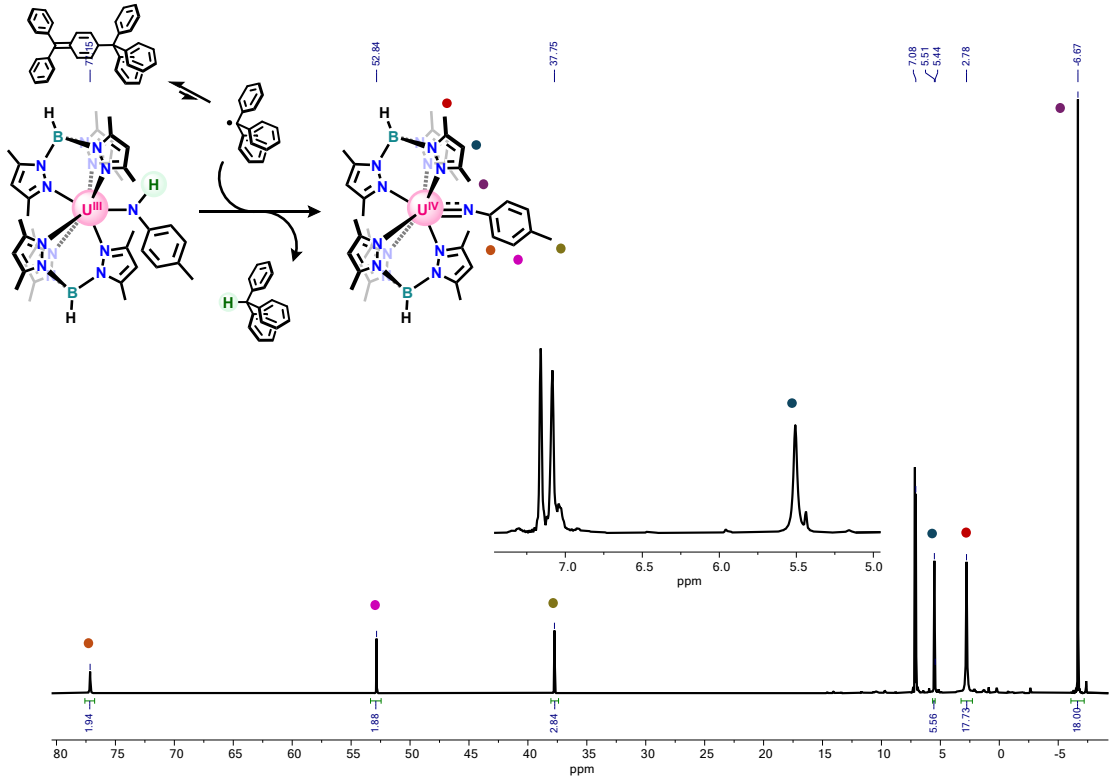

Figure S4. ^{1}H-NMR Spectrum (400.13 MHz, 26 °C, C_6D_6) of the reaction of **1** with Gomberg's Dimer.

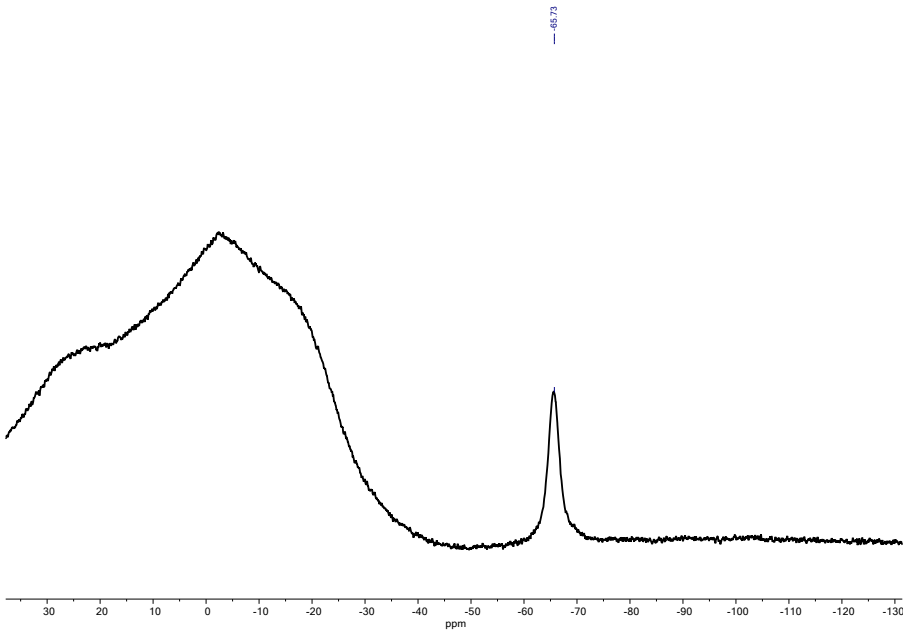

Figure S5. ^{11}B{^{1}H}-NMR Spectrum (128.38 MHz, 26 °C, C_6D_6) of the reaction of **1** with Gomberg's Dimer.

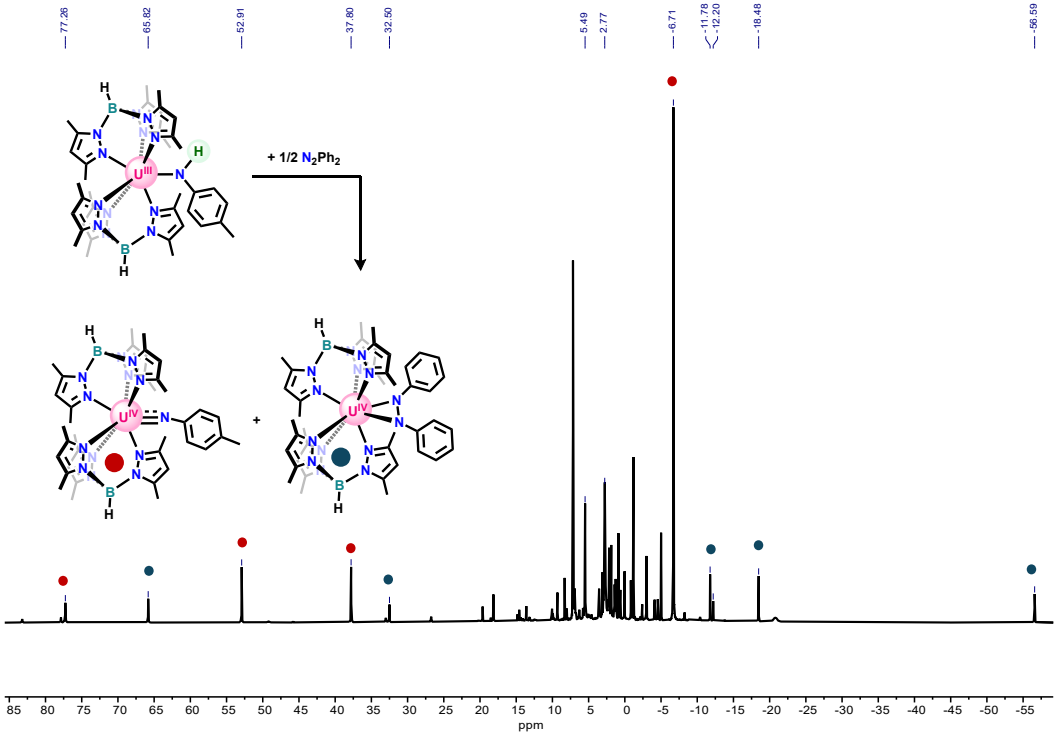

Figure S6. ^{1}H-NMR Spectrum (400.13 MHz, 26 °C, C_6D_6) of the reaction of **1** with azobenzene. Diagnostic peaks for compounds **2** and **3** are marked.

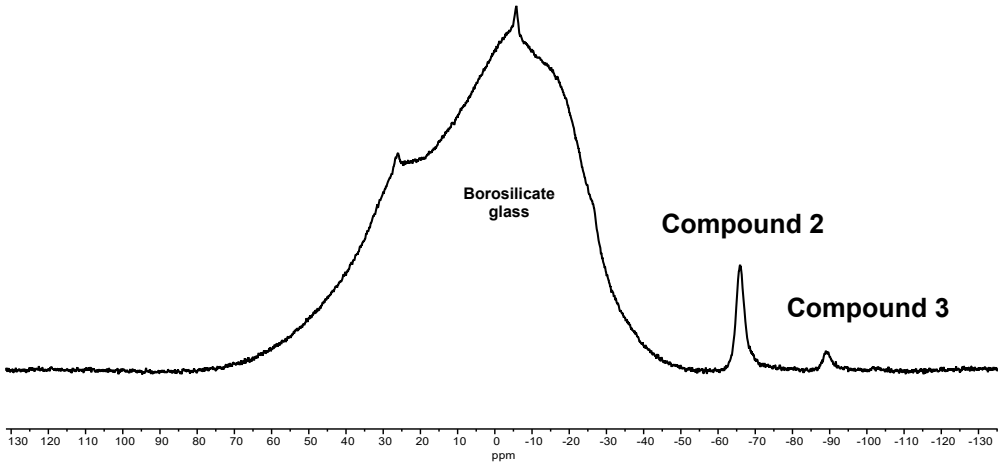

Figure S7. ^{11}B{^{1}H}-NMR Spectrum (128.38 MHz, 26 °C, C_6D_6) of the reaction of **1** with azobenzene.

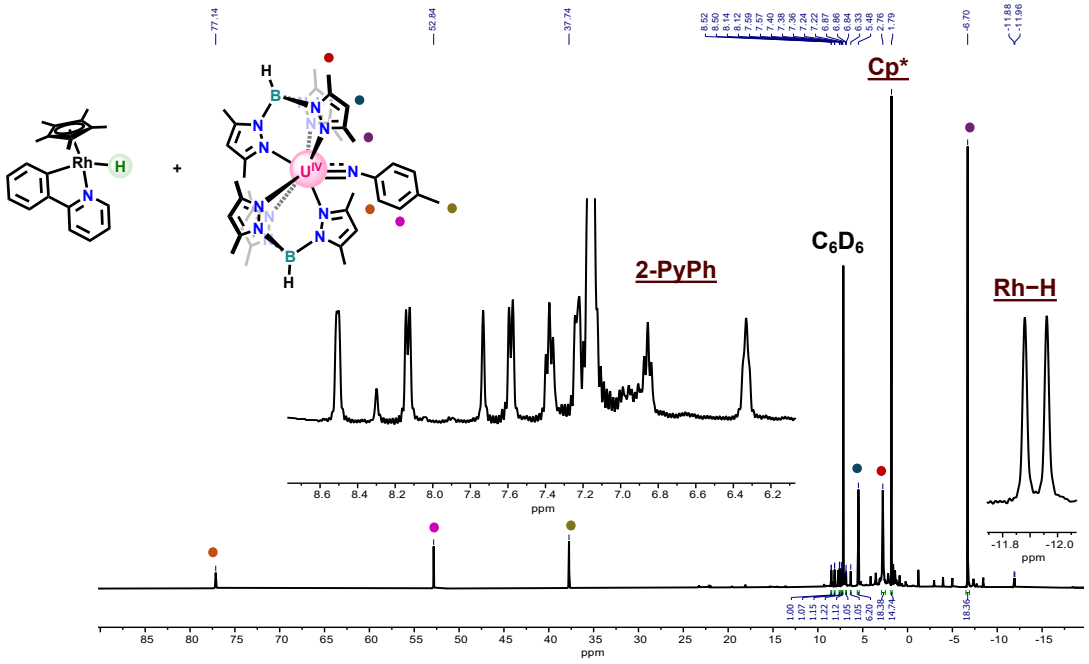

Figure S8. ^{1}H-NMR Spectrum (400.13 MHz, 26 °C, C_6D_6) of the attempted reaction of **2** with the Cp*Rh(2-PyPh)H HAT reagent.

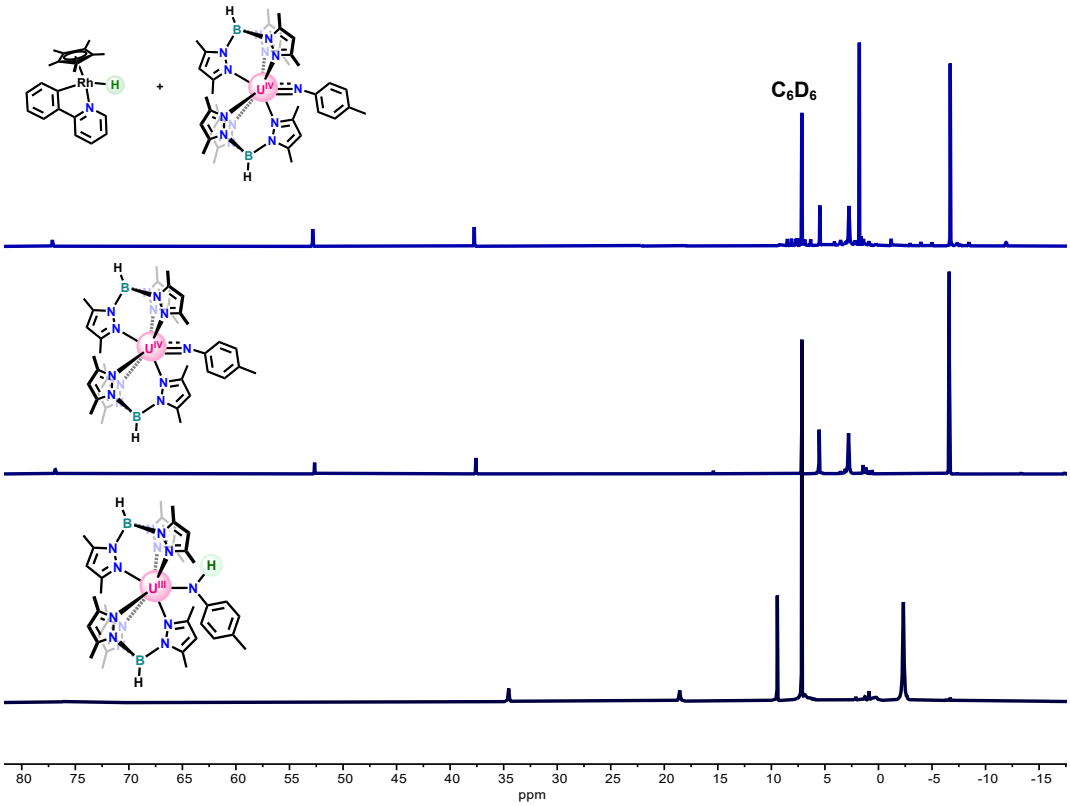

Figure S9. ^{1}H-NMR Spectrum (400.13 MHz, 26 °C, C_6D_6) of the attempted reaction of **2** with the Cp*Rh(2-PyPh)H HAT reagent (top) overlayed with compound **2** (middle) and compound **1** (bottom).

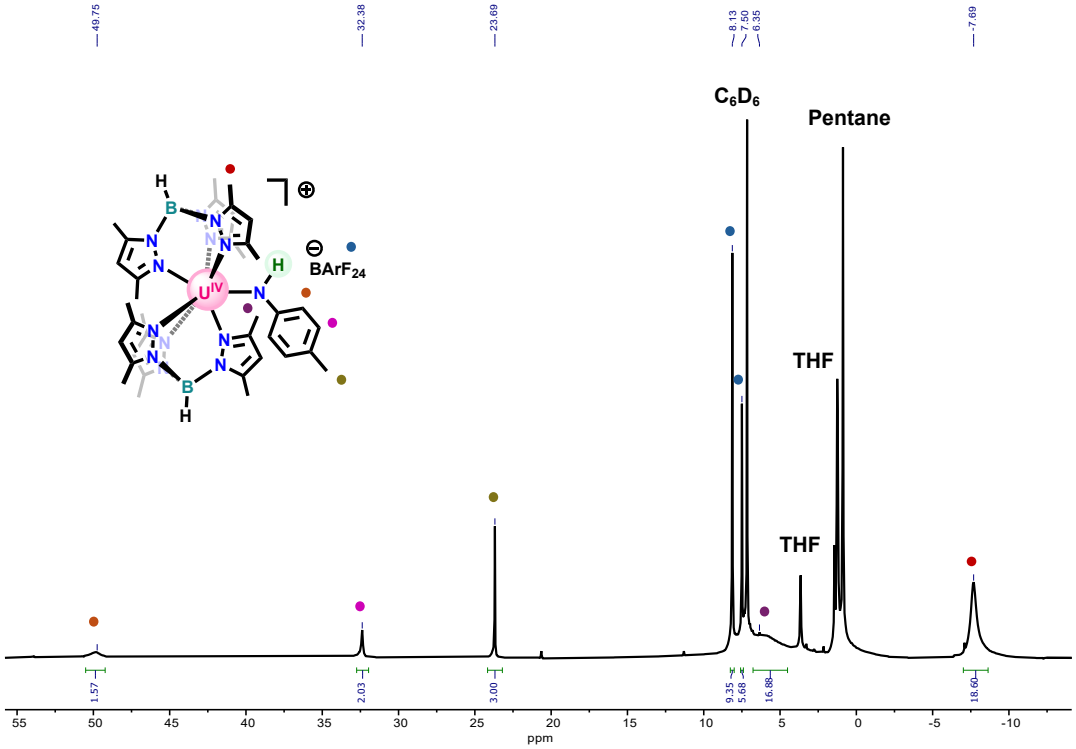

Figure S10. ^{1}H-NMR Spectrum (400.13 MHz, 26 °C, C_6D_6) of **4**.

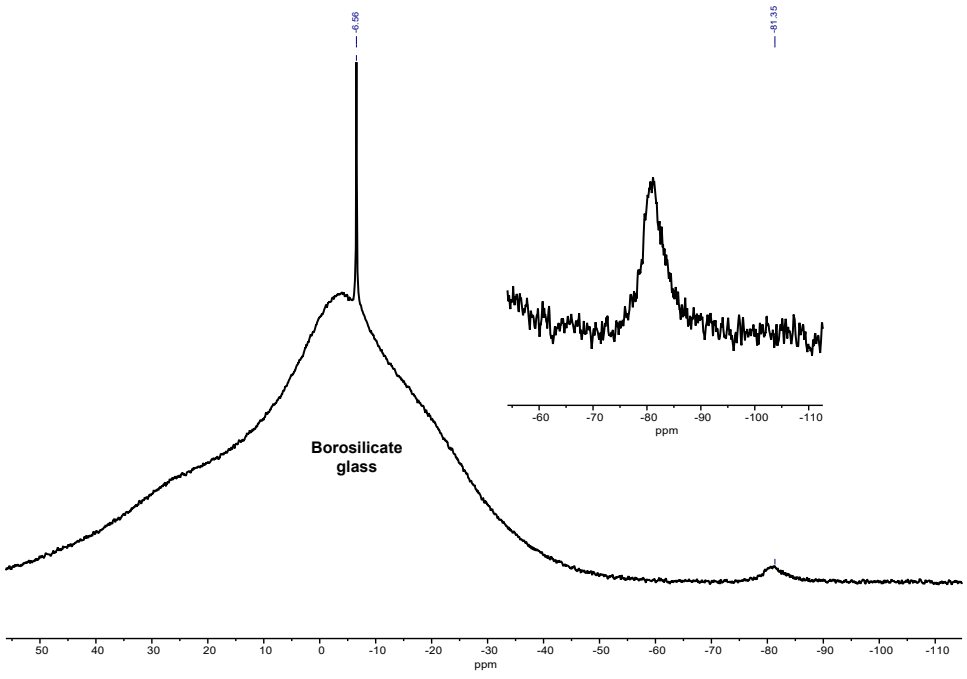

Figure S11. ^{11}B{^{1}H}-NMR Spectrum (128.38 MHz, 26 °C, C_6D_6) of **4**.

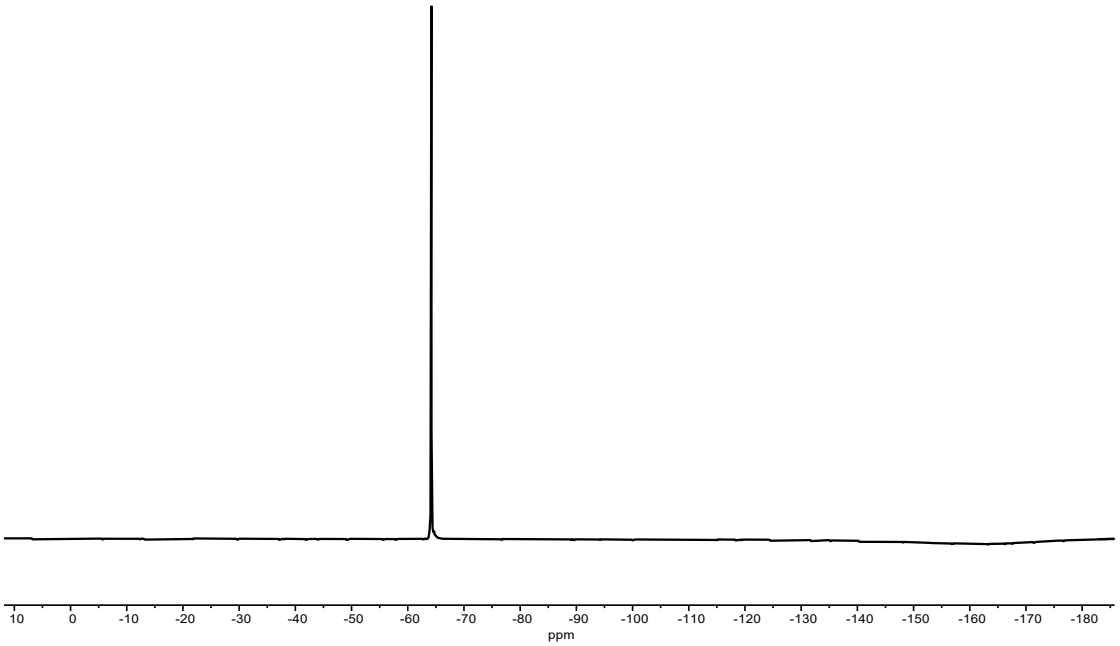

Figure S12. $^{19}F\{^{1}H\}$-NMR (376.50 MHz, 26 °C, C_6D_6) of **4**.

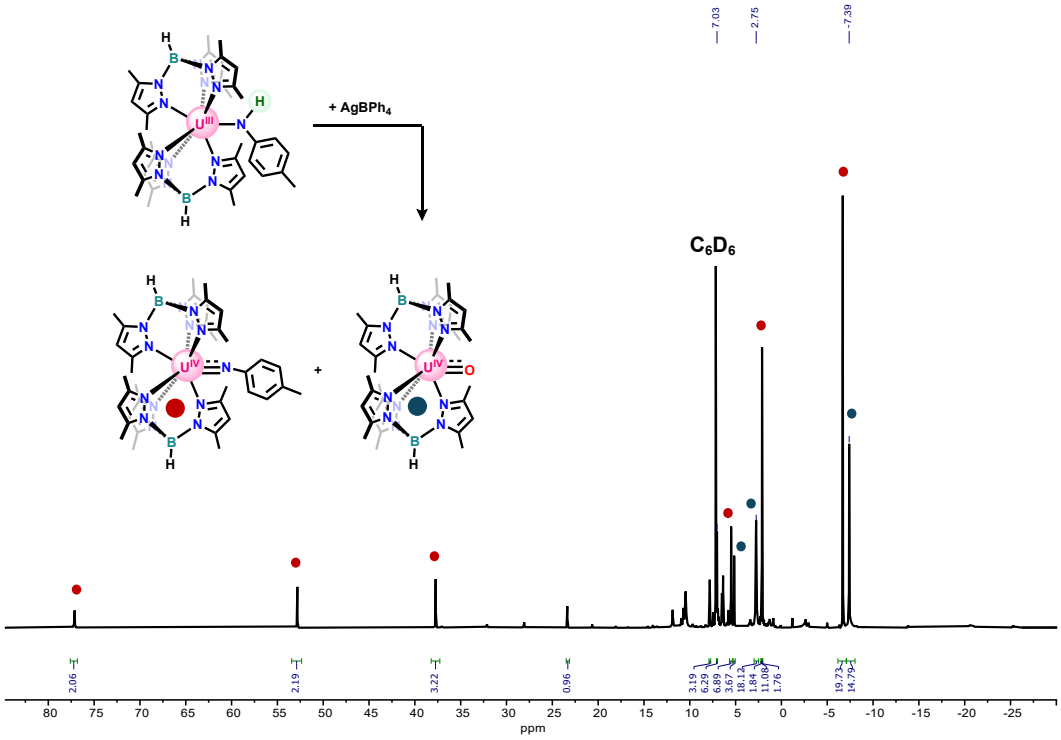

Figure S13. ^{1}H-NMR Spectrum (400.13 MHz, 26 °C, C_6D_6) of the reaction of **1** with $AgBPh_4$.

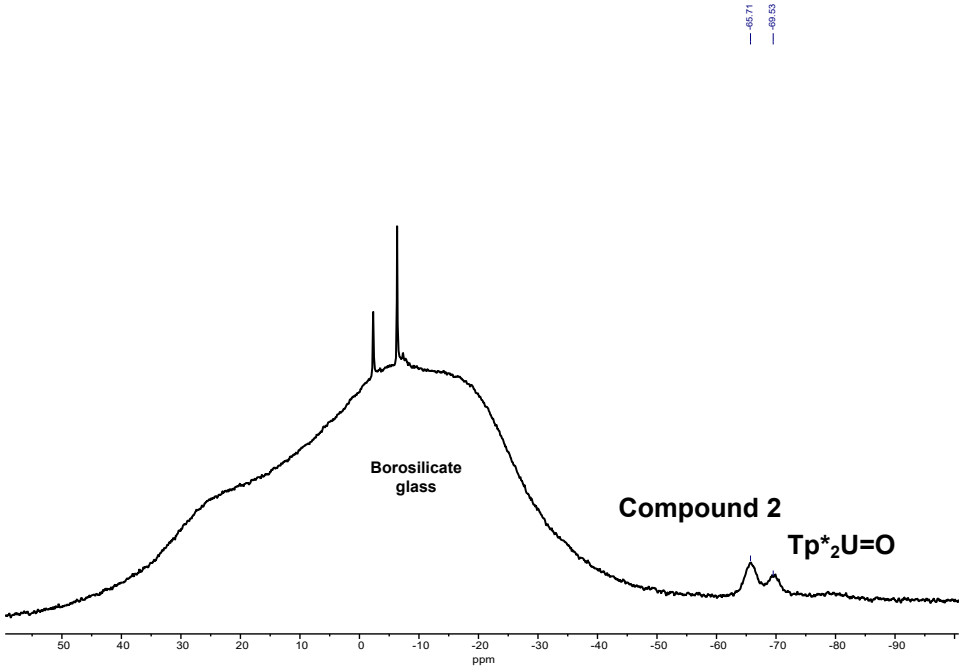

Figure S14. $^{11}B\{^{1}H\}$-NMR Spectrum (128.38 MHz, 26 °C, C_6D_6) of the reaction of **1** with $AgBPh_4$.

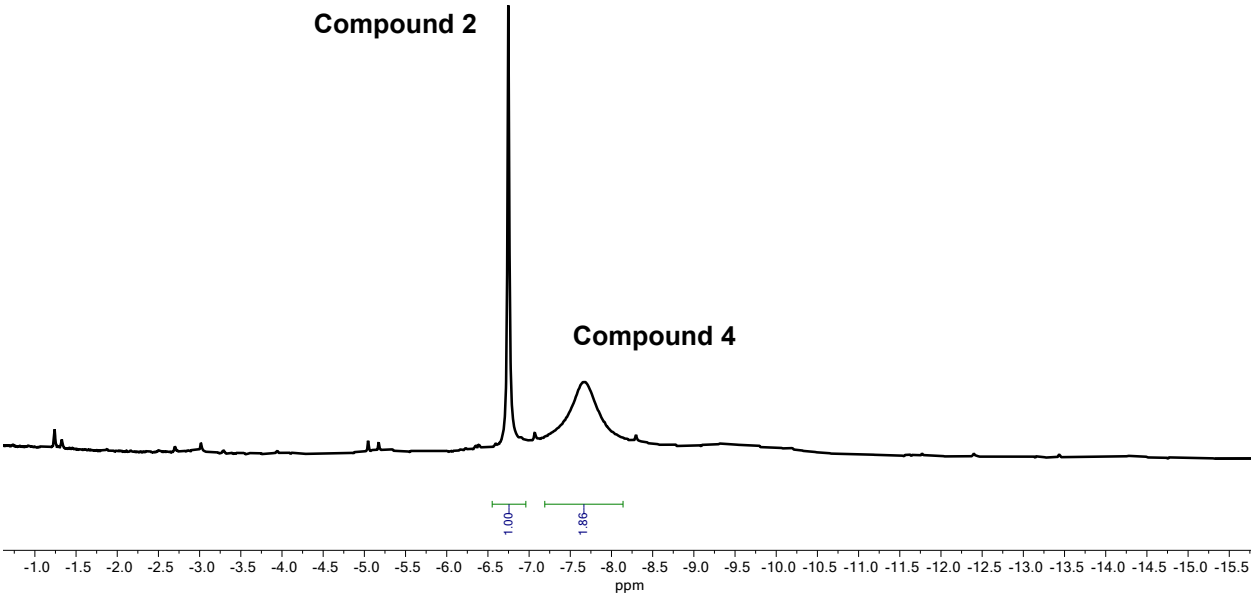

Figure S15. ^{1}H-NMR Spectrum (400.13 MHz, 26 °C, C_6D_6) of the unoptimized reaction of **1** with $[Cp_2Co]BArF_{24}$ resulting in significant formation of **2**.

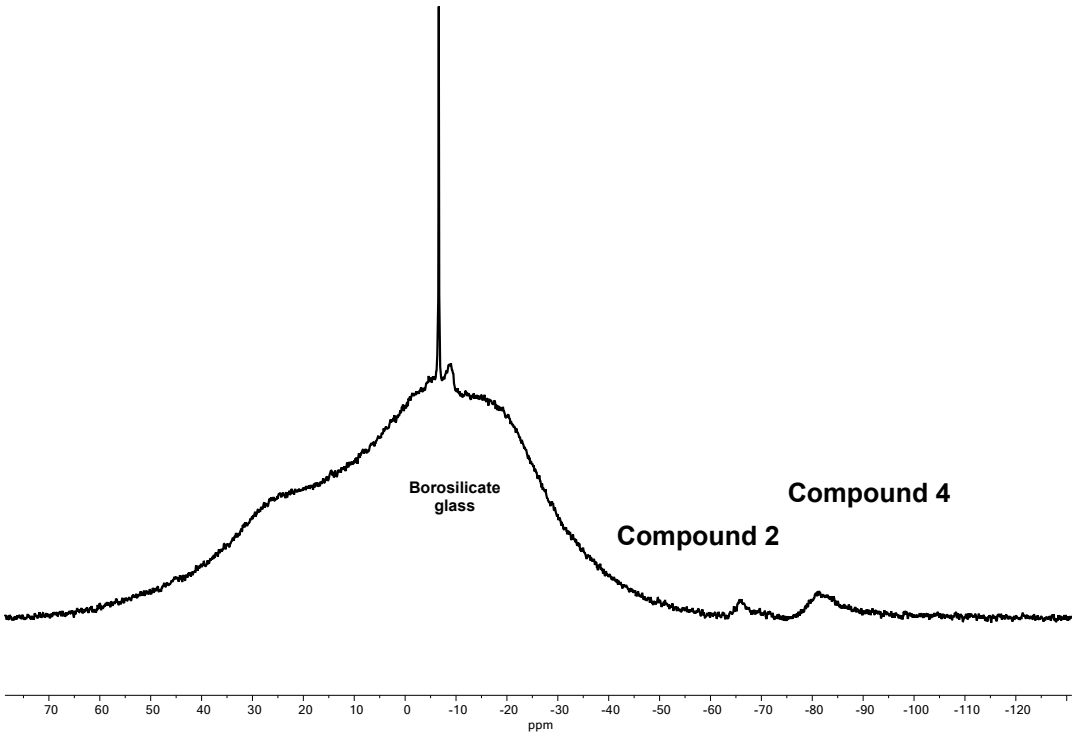

Figure S16. $^{11}B\{^{1}H\}$-NMR Spectrum (128.38 MHz, 26 °C, C_6D_6) of the unoptimized reaction of **1** with $[Cp_2Co]BArF_{24}$ resulting in significant formation of **2**.

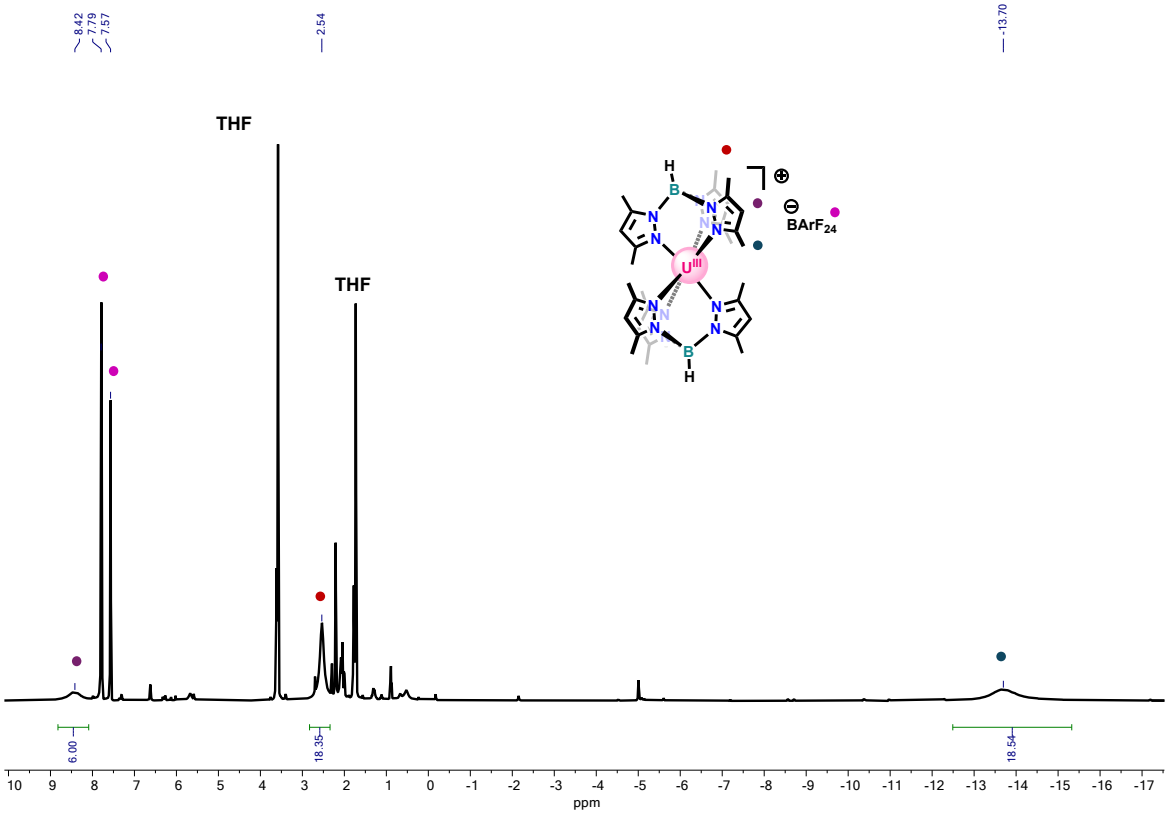

Figure S17. ^{1}H-NMR Spectrum (400.13 MHz, 26 °C, THF-d_8) of **5**.

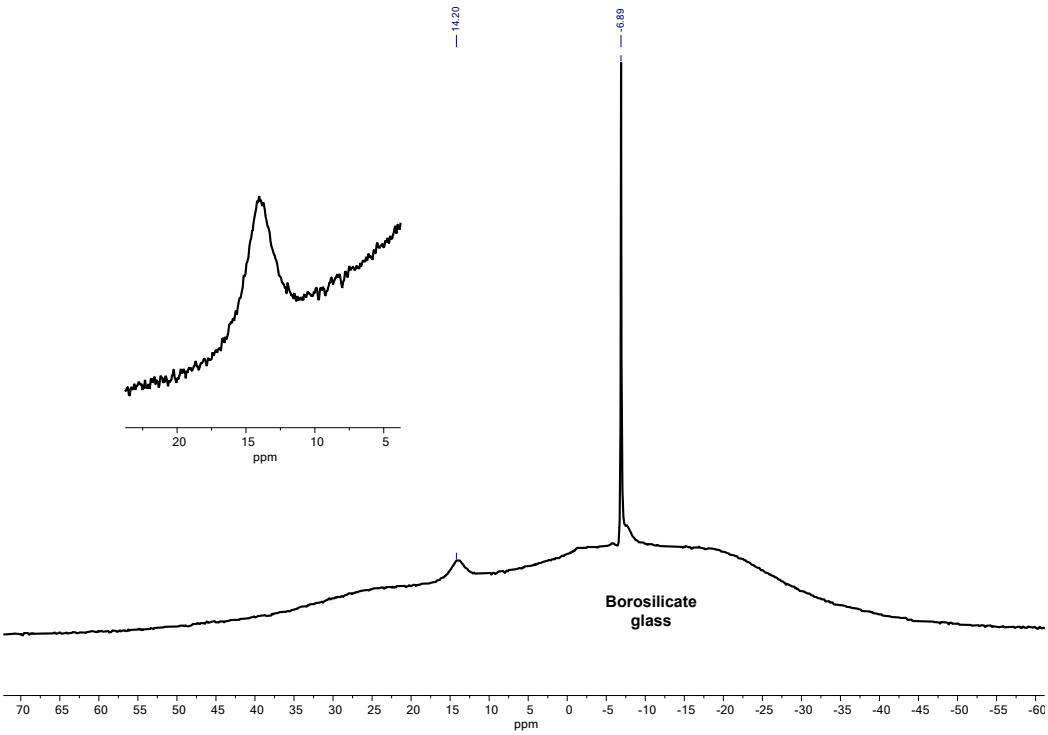

Figure S18. $^{11}B\{^{1}H\}$-NMR (128.38 MHz, 26 °C, THF-d_8) of **5**.

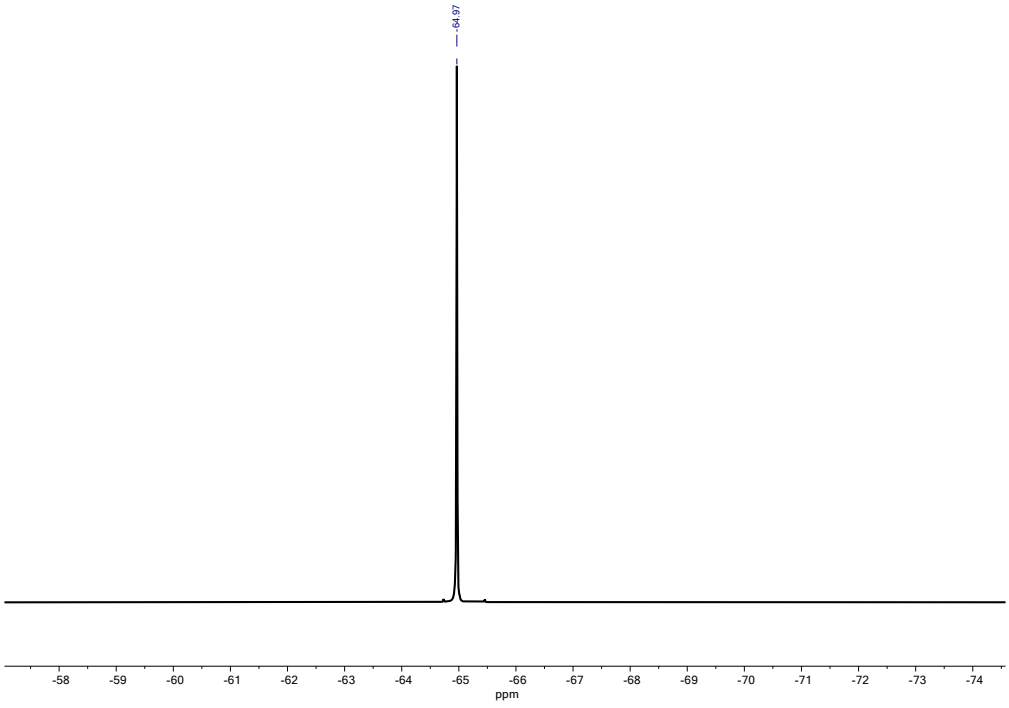

Figure S19. $^{19}F\{^{1}H\}$-NMR (376.50 MHz, 26 °C, THF-d_8) of **5**.

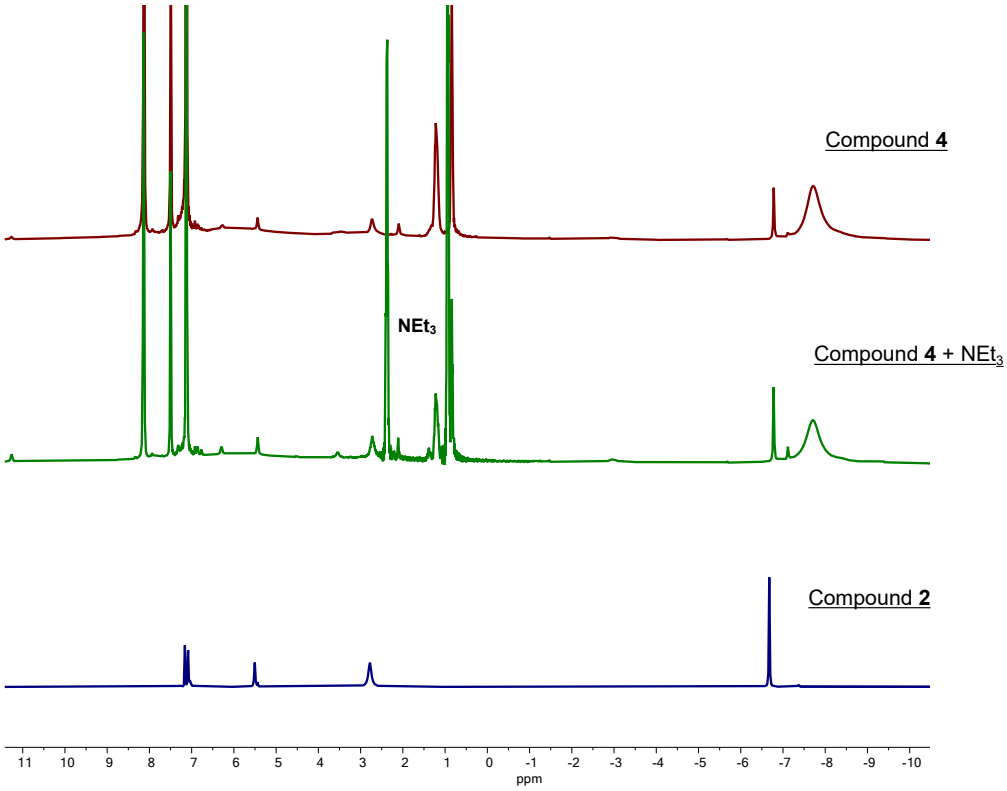

Figure S20. ^{1}H-NMR Spectrum (400.13 MHz, 26 °C, C_6D_6) of the isolated product of **4** with NEt_3 (middle), stacked with **4** (top) and **2** (bottom).

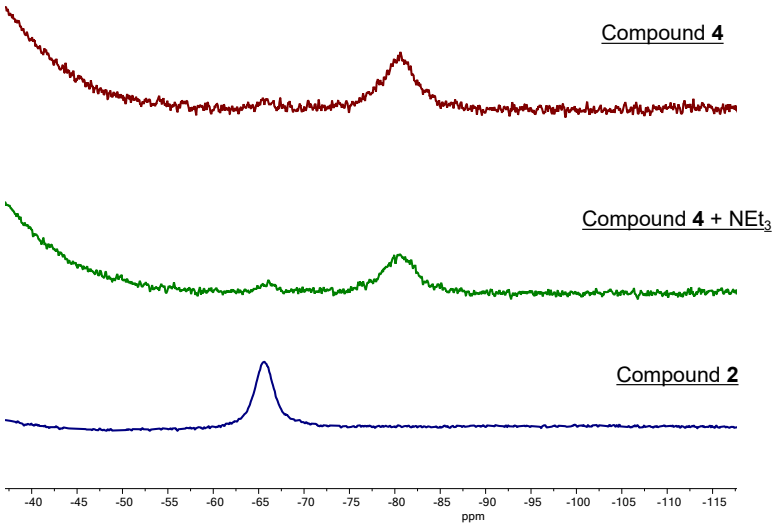

Figure S21. ^{11}B{^{1}H}-NMR Spectrum (128.38 MHz, 26 °C, C_6D_6) of the isolated product of **4** with NEt_3 (middle), stacked with **4** (top) and **2** (bottom).

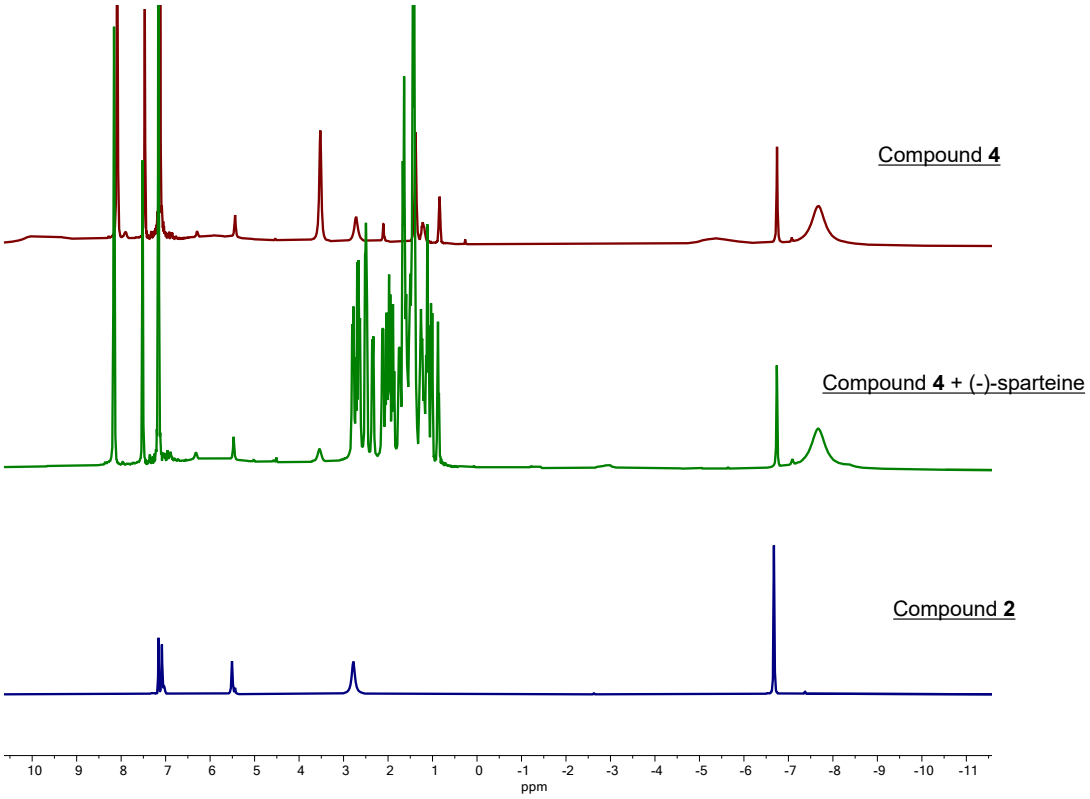

Figure S22. ^{1}H-NMR Spectrum (400.13 MHz, 26 °C, C_6D_6) of the reaction of **4** with (-)-sparteine (middle), stacked with **4** (top) and **2** (bottom).

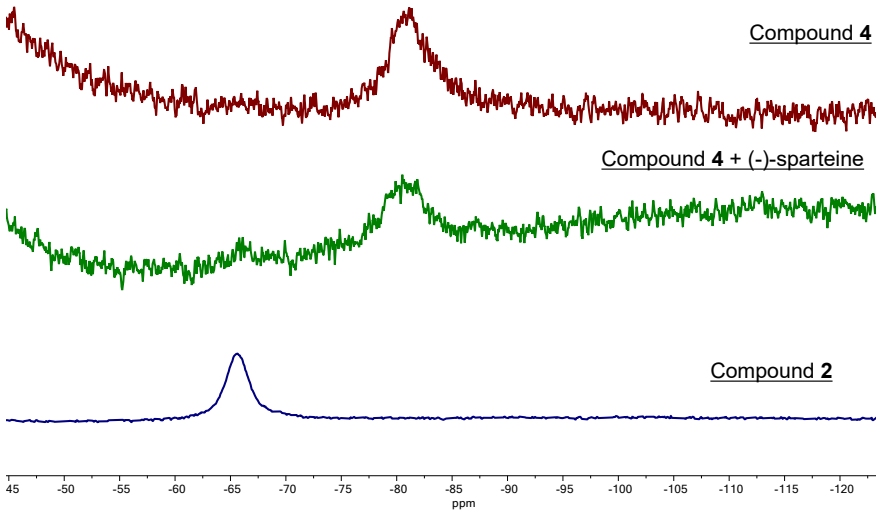

Figure S23. ^{11}B{^{1}H}-NMR Spectrum (128.38 MHz, 26 °C, C_6D_6) of the reaction of **4** with (-)-sparteine (middle), stacked with **4** (top) and **2** (bottom).

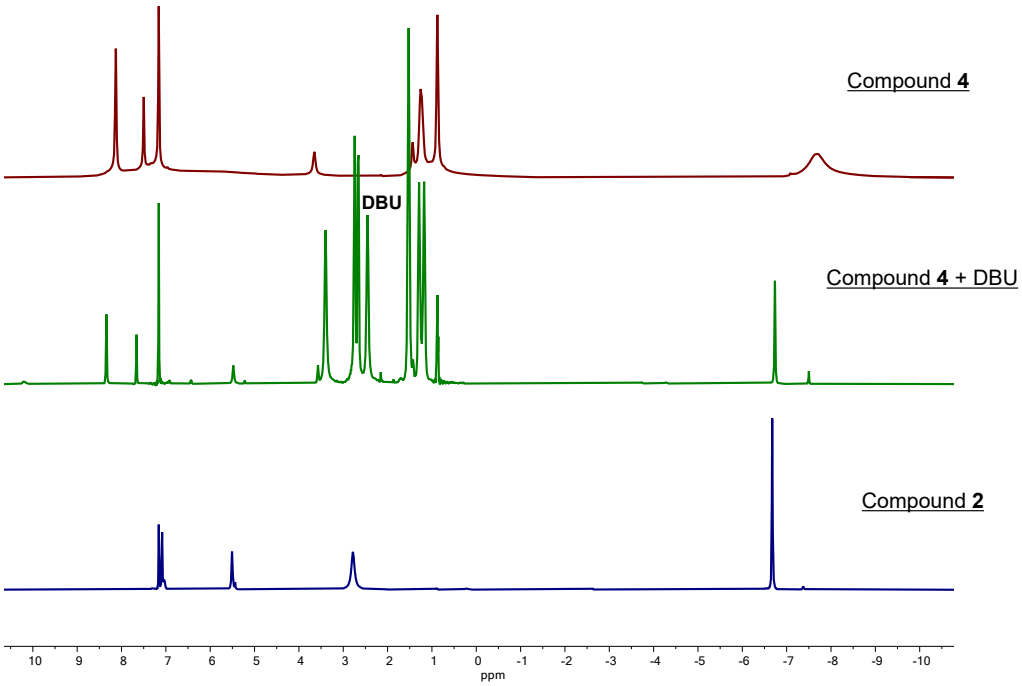

Figure S24. ^{1}H-NMR Spectrum (400.13 MHz, 26 °C, C_6D_6) of the reaction of **4** with DBU (middle), stacked with **4** (top) and **2** (bottom).

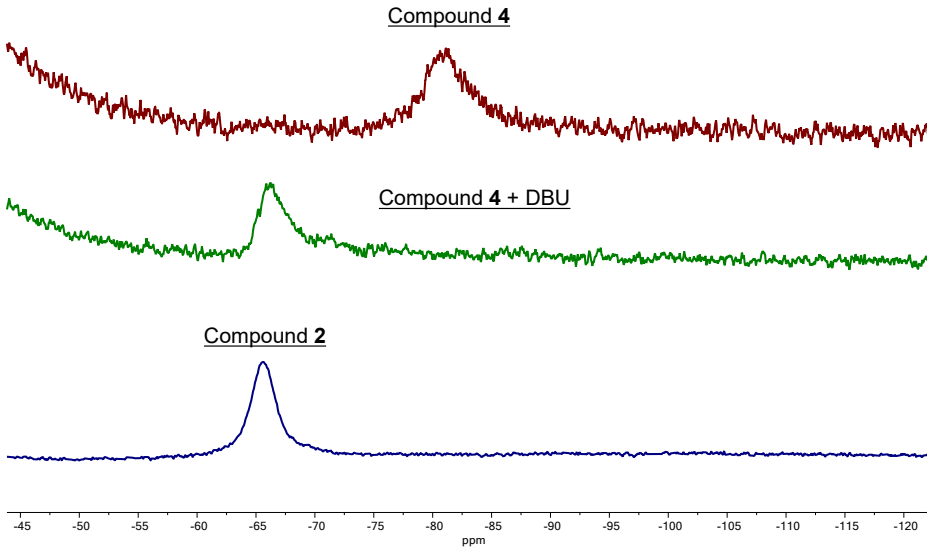

Figure S25. ^{11}B{^{1}H}-NMR Spectrum (128.38 MHz, 26 °C, C_6D_6) of the reaction of **4** with DBU (middle), stacked with **4** (top) and **2** (bottom).

FT-IR Spectroscopic Data.

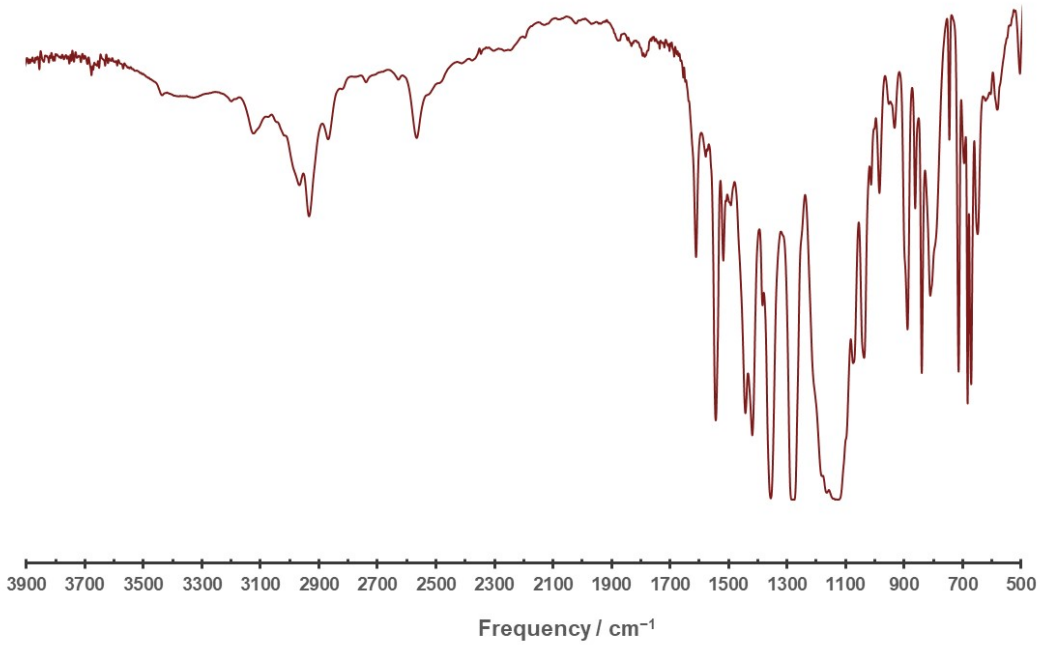

Figure S26. FTIR spectrum of **4** (KBr pellet)

Electronic Spectral Data.

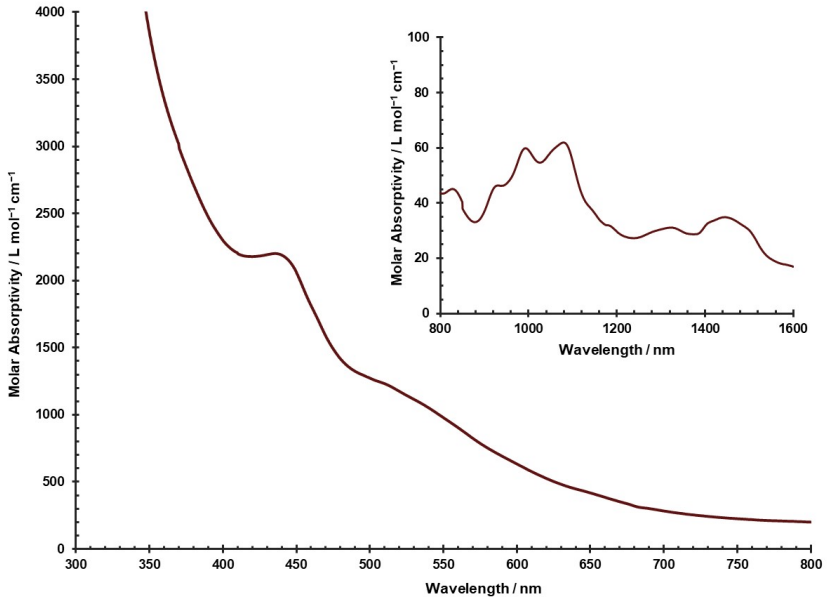

Figure S27. Electronic spectra of **4** for wavelengths ranging from 300-1600 nm. UV/Vis. (300-800) data collected with a concentration of 0.216 mM in THF. NIR (800-1600; inset) was collected with a concentration of 2.16 mM.

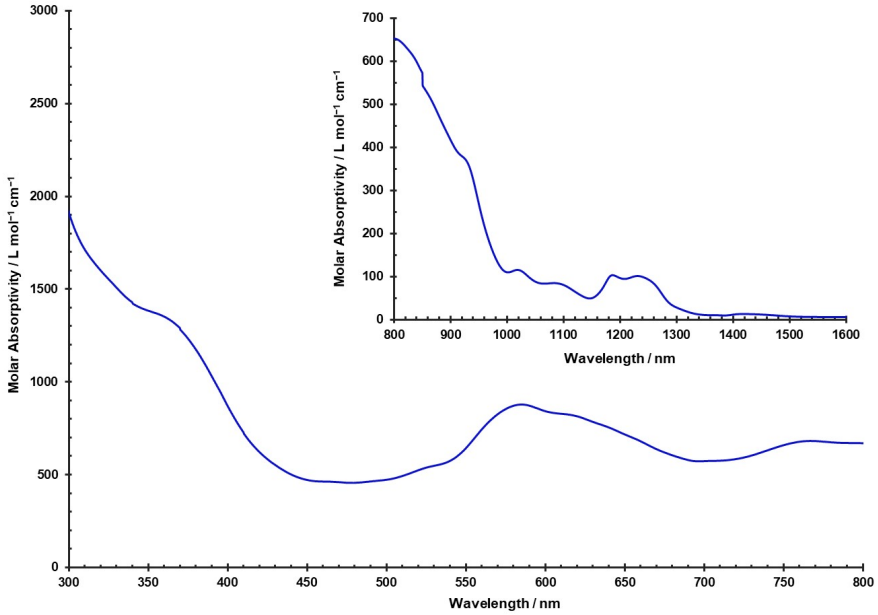

Figure S28. Electronic spectra of **5** for wavelengths ranging from 300-1600 nm. UV/Vis. (300-800) data collected with a concentration of 0.306 mM in THF. NIR (800-1600; inset) was collected with a concentration of 1.33 mM.

Crystallographic Information.

Table 11. Crystal data and structure refinement for 4

CCDC number	2530055
Empirical formula	$C_{78.22}H_{86.13}B_3F_{24}N_{13}U$
Formula weight	1934.83
Temperature [K]	150(2)
Crystal system	triclinic
Space group (number)	$P\bar{1}$ (2)
a [Å]	14.4732(8)
b [Å]	14.7769(9)
c [Å]	21.7868(13)
α [°]	86.256(3)
β [°]	76.813(3)
γ [°]	72.975(3)
Volume [Å^3]	4337.8(4)
Z	2
ρ_{calc} [gcm^{-3}]	1.481
μ [mm^{-1}]	6.151
F(000)	1939
Crystal size [mm^3]	0.038×0.188×0.454

Crystal colour	red brown
Crystal shape	plate
Radiation	CuK_α (λ=1.54178 Å)
2θ range [°]	6.26 to 161.83 (0.78 Å)
Index ranges	−18 ≤ h ≤ 18 −18 ≤ k ≤ 18 −27 ≤ l ≤ 27
Reflections collected	95224
Independent reflections	18668 R_{int} = 0.0822 R_{sigma} = 0.0552
Completeness to θ = 67.679°	100.0
Data / Restraints / Parameters	18668 / 1071 / 1375
Absorption correction T_{min}/T_{max} (method)	0.0780 / 0.6537 (numerical)
Goodness-of-fit on F^2	1.064
Final R indexes [I≥2σ(I)]	R_1 = 0.0426 wR_2 = 0.1062
Final R indexes [all data]	R_1 = 0.0522 wR_2 = 0.1090
Largest peak/hole [eÅ^{-3}]	2.49/−1.06

Refinement details for 4 A pentane solvent molecule's bond lengths were restrained to expected target values (1.55(2) and 1.53(2) Å for C-C bond distances). Another pentane solvent molecule was found to be disordered which was refined using a general disorder model, where the molecules were split over two sets of positions with complimentary occupancy. The disordered moieties were restrained to have similar geometries to the non-disordered pentane molecule (SAME restraint, with a 0.02 Å esd). All chemically equivalent C-C bonds were also restrained to be similar to each other. U_{ij} components of ADPs closer to each other than 2.0Å were restrained to be similar (SIMU restraint, with a 0.01 Å^2 esd). Subject to these conditions, the occupancy ratio refined to 0.67(2) to 0.33(2). Six trifluoromethyl groups were also found to be disordered which were refined using a general disorder model, where each group was split over two sets of positions with complimentary occupancy. The disordered moieties were restrained to have similar geometries to a non-disordered trifluoro methyl group (SAME restraint, with a 0.01 Angstrom esd). U_{ij} components of ADPs closer to each other than 2.0 Å were restrained to be similar (SIMU restraint, with a 0.01 Å^2 esd). All chemically equivalent C-C bonds towards CF_3 groups were also restrained to be similar to each other, and select C-F bonds were restrained to have similar bond lengths (those of C44A, C44B, C53A and C53B). Subject to these conditions, the occupancy ratios refined to 0.861(9) to 0.139(9), 0.701(11) to 0.299(11), 0.452(15) to 0.548(15), 0.909(6) to 0.091(6), 0.629(12) to 0.371(12), and 0.457(13) to 0.543(13). The hydrogen atom bound to nitrogen was placed in an idealized position using an HFIX 43 instruction, which applies a riding model and a refined nitrogen hydrogen bond length. The HFIX 43 command was then removed, and the position of the hydrogen atom was allowed to freely refine. The hydrogen atoms bonded to the borons were located from difference electron density maps and their positions were allowed to refine. The boron hydrogen bond lengths were restrained to a target value of 1.10(2).

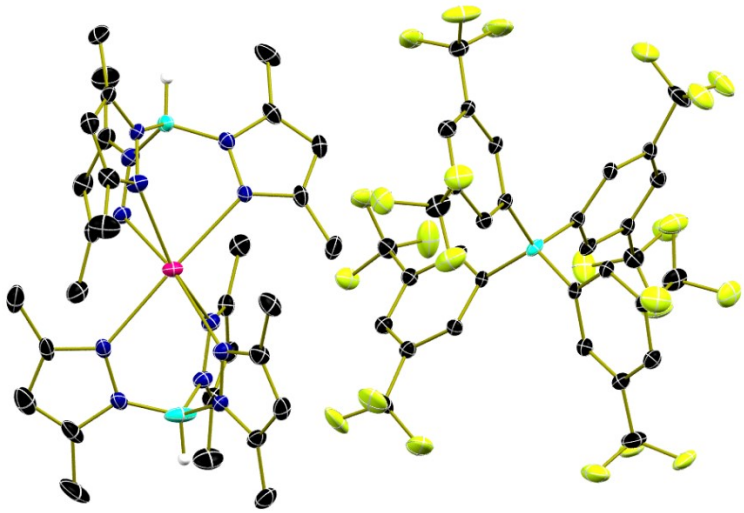

Figure S29. ORTEP representation of the molecular structure of **5**. Thermal ellipsoids are shown at 30% probability. Hydrogen atoms bound to carbon and the $BArF_{24}$ anion are omitted for clarity. Structure only provides connectivity due to poor data quality.

References

1 Y. Sun, R. McDonald, J. Takats, V. W. Day and T. A. Eberspacher, *Inorg. Chem.*, 1994, **33**, 4433–4434.
2 E. M. Matson, W. P. Forrest, P. E. Fanwick and S. C. Bart, *J. Am. Chem. Soc.*, 2011, **133**, 4948–4954.
3 D. Perales, S. A. Ford, S. R. Salpage, T. S. Collins, M. Zeller, K. Hanson and S. C. Bart, *Inorg. Chem.*, 2020, **59**, 11910–11914.
4 N. A. Yakelis and R. G. Bergman, *Organometallics*, 2005, **24**, 3579–3581.
5 D. R. Blechschmidt, A. Lovstedt and S. R. Kass, *Organometallics*, 2022, **41**, 2648–2655.
6 Y. Hu, L. Li, A. P. Shaw, J. R. Norton, W. Sattler and Y. Rong, *Organometallics*, 2012, **31**, 5058–5064.
7 N. J. Lin, K. L. Gullett, U. K. Muna, R. Galloway, M. Zeller and S. C. Bart, *Organometallics*, 2025, **44**, 289–299.
8 A. Bismuto, P. Müller, P. Finkelstein, N. Trapp, G. Jeschke and B. Morandi, *J. Am. Chem. Soc.*, 2021, **143**, 10642–10648.
9 Bruker, SAINT, V8.41, Bruker AXS SE, Karlsruhe, Germany., .
10 L. Krause, R. Herbst-Irmer, G. M. Sheldrick and D. Stalke, *J. Appl.Crystallogr.*, 2015, 48, 3–10.
11 G. Sheldrick, *Acta Crystallogr. A*, 2015, 71, 3–8.
12 G. Sheldrick, *Acta Crystallogr. C*, 2015, 71, 3–8.
13 C. R. Groom, I. J. Bruno, M. P. Lightfoot and S. C. Ward, *Acta Crystallogr. B*, 2016, 72, 171–179.
14 C. J. Tatebe, M. Zeller and S. C. Bart, *Inorg. Chem.*, 2017, **56**, 1956–1965.
15 J. J. Kiernicki, R. F. Higgins, S. J. Kraft, M. Zeller, M. P. Shores and S. C. Bart, *Inorg. Chem.*, 2016, **55**, 11854–11866.
16 S. J. Kraft, J. Walensky, P. E. Fanwick, M. B. Hall and S. C. Bart, *Inorg. Chem.*, 2010, **49**, 7620–7622.